

Statistica Sinica Preprint No: SS-2018-0476

Title	Estimating large precision matrices via modified Cholesky decomposition
Manuscript ID	SS-2018-0476
URL	http://www.stat.sinica.edu.tw/statistica/
DOI	10.5705/ss.202018.0476
Complete List of Authors	Kyoungjae Lee and Jaeyong Lee
Corresponding Author	Kyoungjae Lee
E-mail	leekjstat@gmail.com
Notice: Accepted version subject to English editing.	

ESTIMATING LARGE PRECISION MATRICES VIA MODIFIED CHOLESKY DECOMPOSITION

Kyoungjae Lee and Jaeyong Lee

The University of Notre Dame and Seoul National University

Abstract: We introduce the k -banded Cholesky prior for estimating a high-dimensional bandable precision matrix via the modified Cholesky decomposition. The bandable assumption is imposed on the Cholesky factor of the decomposition. We obtain the P-loss convergence rate (Lee and Lee, 2018) under the spectral norm and the matrix ℓ_∞ norm and minimax lower bounds. Since the P-loss convergence rate is stronger than the posterior convergence rate, the rates obtained are also posterior convergence rates. Furthermore, when the true precision matrix is a k_0 -banded matrix with some finite k_0 , we obtain the minimax rate. The established convergence rates for bandable precision matrices are slightly slower than minimax lower bounds, but these are the fastest rates among the existing Bayesian approaches. The performance of the proposed method was better than or comparable to that of the other competitive estimators in our simulation study.

Key words and phrases: Modified Cholesky decomposition, P-loss Convergence rate, precision matrix.

1. Introduction

In recent years, it is common that the number of variables p of a data set is much larger than their sample size n . Examples of such high-dimensional data sets arise from genomics, climatology, fMRI and neuroimaging, to name just a few. In this paper, we concentrate on the estimation of the precision matrix, the inverse of the covariance matrix, for a high-dimensional data.

When the number of variables p tends to infinity as $n \rightarrow \infty$ and is possibly larger than n , the traditional sample covariance fails to converge to the true covariance matrix (Johnstone and Lu, 2009). Thus, it is necessary to assume certain constraints on the covariance to get a consistent estimator under the ultra high-dimensional setting, $\log p = o(n)$. The constraint on the covariance matrix includes the sparse, bandable assumption or lower-dimensional structure such as sparse spiked covariance and factor model. The minimax convergence rates under the sparsity or bandable assumption on a covariance/precision matrix were established by Bickel and Levina (2008a), Bickel and Levina (2008b), Cai et al. (2010), Cai and Zhou (2012a), Cai and Zhou (2012b), Xue and Zou (2013), Cai et al. (2016) and Hu and Negahban (2017), to just name a few. Bickel and Levina (2008b) and Verzelen (2010) obtained convergence rates for the precision matrices

under the sparsity or bandable assumption via Cholesky decomposition. The convergence rates under lower-dimensional structures of covariance matrix such as factor model (Fan et al., 2008) and sparse spiked covariance model (Cai et al., 2015) were also explored. Cai et al. (2015) and Fan et al. (2015) derived the minimax convergence rates for the functionals of the covariance matrices. Cai et al. (2016) provided a comprehensive review on the convergence rate for large matrices.

From the Bayesian side, the posterior convergence rates for large covariance or precision matrices have been investigated, but there are relatively few works available in high-dimensional settings. Banerjee and Ghosal (2015) showed the posterior convergence rate for the precision matrix under the sparsity assumption. They used a mixture prior for off-diagonal elements of the precision matrix to assign exactly zero. To estimate bandable precision matrices, Banerjee and Ghosal (2014) utilized the G -Wishart prior on the precision matrix and established the posterior convergence rate. Xiang et al. (2015) extended the result of Banerjee and Ghosal (2014) to decomposable graphical models which contains the bandable precision matrices as a special case. Pati et al. (2014) considered the posterior convergence rate for covariance estimation via the sparse factor model. They obtained nearly optimal rates, the minimax rates with $(\log n)^{1/2}$ factor when

the number of true factors is bounded. The optimal posterior convergence rate for covariance matrices under the sparse spiked covariance model was derived by Gao and Zhou (2015). Cao et al. (2016) considered the sparse Cholesky factor of the precision matrix and proved the strong model selection consistency and convergence rate. The above results assumed the ultra high-dimensional setting, $\log p = o(n)$, or its variants. Recently, Gao and Zhou (2016) derived Bernstein-von Mises theorems for functionals of the covariance matrix as well as its inverse, under conditions such as $p = o(n)$ or $p^3 = o(n)$.

Lee and Lee (2018) proposed a new decision theoretical framework for prior selection and obtained the Bayesian minimax rate of the unconstrained covariance matrix under the spectral norm for all rates of p . The Bayesian minimax rates under the Frobenius norm, the Bregman divergence and squared log-determinant loss were also obtained when $p \leq n^{1/2}$ or $p = o(n)$. They showed that when $p > n/2$, there is no better prior than the point mass prior δ_{I_p} in terms of the induced posterior convergence rate. It implies that a certain restriction on the covariance or precision matrix is needed for consistent estimation.

In this paper, we consider a class of bandable precision matrices via the modified Cholesky decomposition under the ultra high-dimensional set-

ting, and derive the P-loss convergence rates under the spectral norm and matrix ℓ_∞ norm. Since the P-loss convergence rate implies the traditional posterior convergence rate, the P-loss convergence rate can be considered as the posterior convergence rate. The bandable assumption is imposed on the lower triangular matrix from the modified Cholesky decomposition, which is called the Cholesky factor. Bickel and Levina (2008b) used a similar assumption and their parameter space is a special case of ours. Our work is also closely related to the works of Banerjee and Ghosal (2014) and Xiang et al. (2015) for they considered the bandable precision matrices. We emphasize that when the true precision matrix is a k_0 -banded with some finite k_0 , we obtain the minimax rate. Furthermore, when the true precision matrix is bandable, the convergence rate obtained in this paper is faster than those obtained in the above papers. To the best of our knowledge, this is the fastest rate for the bandable precision matrices among existing Bayesian methods. Although our parameter space is not exactly same as that of Banerjee and Ghosal (2014), they are closely related. Proposition 1 describes the close relationship between them. This paper is also related to Cao et al. (2016), but they considered only the sparse Cholesky factor whose elements are exactly zero except only a few. Thus, it does not cover the class of bandable Cholesky factors considered in this paper. Fur-

thermore, we show minimax lower bounds for precision matrices under the bandable assumption on the Cholesky factor. The lower bounds are derived under the spectral norm as well as matrix ℓ_∞ norm. Recently, Liu and Ren (2017) have obtained sharper lower bound for the spectral norm under the bandable assumption on the Cholesky factor, concurrently with our work.

The rest of the paper is organized as follows. In section 2, we define our model, matrix norms, the parameter class and the decision theoretic prior selection. The convergence rates for precision matrices under the spectral norm and matrix ℓ_∞ norm are shown in section 3. In section 4, the practical choice of the bandwidth is proposed, and we conduct a simulation study in section 5. Discussion is given in section 6, and the proofs of the main results are in Supplementary material.

2. Preliminaries

2.1 Norms and Notations

For any constants a and b , $a \vee b$ and $a \wedge b$ denotes the maximum and minimum of a and b , respectively. For any positive sequences a_n and b_n , we denote $a_n = o(b_n)$ if $a_n/b_n \rightarrow 0$ as $n \rightarrow \infty$. We denote $a_n \asymp b_n$ if there exist positive constants C_1 and C_2 such that $C_1 \leq a_n/b_n \leq C_2$ for all sufficiently large n , and $a_n \lesssim b_n$ if there exists a positive constant C such

2.2 The Model and the Prior

that $a_n \leq Cb_n$ for all sufficiently large n . For any $p \times p$ matrix A , $\lambda_{\min}(A)$ and $\lambda_{\max}(A)$ denote the minimum and maximum eigenvalue of the matrix A , respectively.

For any p -dimensional vector a , we define vector norms as follows: $\|a\|_1 := \sum_{i=1}^p |a_i|$, $\|a\|_2 := (\sum_{i=1}^p a_i^2)^{1/2}$ and $\|a\|_{\max} := \max_{1 \leq i \leq p} |a_i|$. With these norms, we define the operator norms for matrices. Let $A = (a_{ij})$ be a $p \times p$ matrix. The spectral norm (or matrix ℓ_2 norm) is defined by

$$\|A\| := \sup_{\substack{x \in \mathbb{R}^p \\ \|x\|_2=1}} \|Ax\|_2 = (\lambda_{\max}(A^T A))^{1/2}.$$

We define the matrix ℓ_1 norm, matrix ℓ_∞ norm and Frobenius norm by

$$\begin{aligned} \|A\|_1 &:= \sup_{\substack{x \in \mathbb{R}^p \\ \|x\|_1=1}} \|Ax\|_1 = \max_j \sum_{i=1}^p |a_{ij}|, \\ \|A\|_\infty &:= \sup_{\substack{x \in \mathbb{R}^p \\ \|x\|_{\max}=1}} \|Ax\|_{\max} = \max_i \sum_{j=1}^p |a_{ij}|, \\ \|A\|_F &:= \left(\sum_{i=1}^p \sum_{j=1}^p a_{ij}^2 \right)^{1/2}, \end{aligned}$$

respectively. The max norm for matrices is defined by $\|A\|_{\max} := \max_{i,j} |a_{ij}|$.

2.2 The Model and the Prior

Suppose we observe a data set from the p -dimensional normal distribution

$$X_1, \dots, X_n \stackrel{iid}{\sim} N_p(0, \Omega_n^{-1}), \quad (2.1)$$

2.2 The Model and the Prior

where Ω_n is a $p \times p$ positive definite matrix. We assume that $p = p_n$ is a function of n increasing to ∞ as $n \rightarrow \infty$. Let $\mathbf{X}_n = (X_1, \dots, X_n)^T$ and $\Omega_{0,n}$ be the $n \times p$ data matrix and $p \times p$ true precision matrix, respectively.

For a $p \times p$ positive definite matrix Ω_n , the modified Cholesky decomposition (MCD) guarantees that there uniquely exist a lower triangular matrix $A_n = (a_{jl})$ and a diagonal matrix $D_n = \text{diag}(d_j)$ such that

$$\Omega_n = (I_p - A_n)^T D_n^{-1} (I_p - A_n), \quad (2.2)$$

where $a_{jj} = 0$ and $d_j > 0$ for all $j = 1, \dots, p$. The MCD has a nice autoregressive interpretation which enables simple and effective inference. Consider a latent variable $\epsilon \sim N_p(0, D_n)$ and a random vector $Y \sim N_p(0, \Omega_n^{-1})$, and note that the relationship $(I_p - A_n)Y \stackrel{d}{=} \epsilon$ holds because they have the same distributions. By this fact, the model (2.1) with a precision matrix (2.2) is equivalent to the following autoregressive model

$$X_{\cdot,1} | d_1 \sim N_n(0, d_1 I_n), \quad (2.3)$$

$$X_{\cdot,j} | a_j, d_j, X_{\cdot,1:(j-1)} \sim N_n(X_{\cdot,1:(j-1)} a_j, d_j I_n), \quad j = 2, \dots, p,$$

where $a_j = (a_{j1}, \dots, a_{j,j-1})^T \in \mathbb{R}^{j-1}$, and $X_{\cdot,j} \in \mathbb{R}^n$ and $X_{\cdot,1:(j-1)} \in \mathbb{R}^{n \times (j-1)}$ are sub-matrices of \mathbf{X}_n consisting of the j th column and the $1, \dots, (j-1)$ th columns, respectively. We denote the sub-matrix of \mathbf{X}_n consisting of a, \dots, b th columns by $X_{\cdot,a:b}$ for any positive integer $a \leq b$. With slight abuse

2.2 The Model and the Prior

of notation, if $a \leq 0$ and $b > 0$, $X_{.,a:b} := X_{.,(a \vee 1):b} = X_{.,1:b}$ to define a proper column position. The zero-pattern in the Cholesky factor A_n and the model (2.3) rely on the order of variables. In this paper, we assume that there is a known natural ordering of variables, which has been commonly assumed in literature including Bickel and Levina (2008b), Shojaie and Michailidis (2010), Khare et al. (2016), Banerjee and Ghosal (2014) and Cao et al. (2016).

Bickel and Levina (2008b) approximated the precision matrix by considering only k closest regressors in the regression interpretation (2.3), which is the same as assuming the lower triangular matrix A_n in the modified Cholesky decomposition to be the k -banded lower triangular matrix. This approximation assumes that based on the given ordering of variables, only k closest previous variables affect the current variable. Note that the resulting precision matrix $\Omega_n = (I_p - A_n)^T D_n^{-1} (I_p - A_n)$ also becomes a k -banded matrix.

In this paper, we suggest the following prior

$$\begin{aligned} \pi(a_{jl}) &\propto 1, \quad l = (j - k) \vee 1, \dots, j - 1, \text{ and } \pi(a_{jl}) = \delta_0, \text{ otherwise,} \\ \pi(d_j) &\propto d_j^{-\nu_0/2-1} I(0 < d_j < M), \quad j = 1, \dots, p, \end{aligned} \tag{2.4}$$

for some non-negative constants M and ν_0 , and ν_0 can be dependent on n . δ_0 is the Dirac measure at 0. Note that the degenerate prior of a_{jl} when

2.2 The Model and the Prior

$l < (j - k) \vee 1$ is due to the k -banded Cholesky factor assumption. We call the prior (2.4) the k -banded Cholesky (k -BC) prior. The appropriate condition on M and ν_0 will be discussed in section 3. The prior (2.4) leads to the following joint posterior distribution,

$$d_j \mid \mathbf{X}_n \stackrel{ind}{\sim} IG^{Tr} \left(d_j \mid \frac{n_j}{2}, \frac{n}{2} \widehat{d}_{jk}, d_j \leq M \right), \quad j = 1, \dots, p, \quad (2.5)$$

$$a_j^{(k)} \mid d_j, \mathbf{X}_n \stackrel{ind}{\sim} N_{j-1 \wedge k} \left(a_j^{(k)} \mid \widehat{a}_j^{(k)}, d_j (X_{\cdot, (j-k):(j-1)}^T X_{\cdot, (j-k):(j-1)})^{-1} \right) \quad j = 2, \dots, p,$$

where $n_j = n + \nu_0 - (j - 1 \wedge k) - 4$, $a_j^{(k)} = (a_{j, (j-k \vee 1)}, \dots, a_{j, j-1})^T$,

$$\widehat{a}_j^{(k)} = (X_{\cdot, (j-k):(j-1)}^T X_{\cdot, (j-k):(j-1)})^{-1} X_{\cdot, (j-k):(j-1)}^T X_{\cdot, j}, \quad (2.6)$$

$$\widehat{d}_{jk} = n^{-1} X_{\cdot, j}^T (I_n - X_{\cdot, (j-k):(j-1)} (X_{\cdot, (j-k):(j-1)}^T X_{\cdot, (j-k):(j-1)})^{-1} X_{\cdot, (j-k):(j-1)}^T) X_{\cdot, j}$$

for $j = 2, \dots, p$, and $\widehat{d}_{1k} = n^{-1} \|X_{\cdot, 1}\|_2^2$. We denote $IG^{Tr}(X \mid a, b, A)$ as the truncated version of $IG(X \mid a, b)$ on support A , where $IG(X \mid a, b)$ is the density function of the inverse-gamma random variable X whose shape and rate parameters are a and b , respectively. $N_p(X \mid \mu, \Sigma)$ is the density function of the p -dimensional normal random variable X whose mean vector and covariance matrix are μ and Σ , respectively.

Remark 1. The main results in section 3 still hold for the prior

$$a_j^{(k)} \mid d_j \stackrel{ind}{\sim} N_{j-1 \wedge k} (m_j, d_j B_j), \quad j = 2, \dots, p \quad (2.7)$$

with certain bounded conditions on $\|m_j\|_2$ and $\|B_j^{-1}\|$. It contains the prior (2.4) as a special case with $m_j = 0$ and $B_j = \text{diag}(b = \infty)$. However, we

2.3 Parameter Class

omitted proofs and represented only results with the prior (2.4) for the simplicity of notation.

Remark 2. The prior for d_j has a compact support for a technical reason to deal with the P-loss defined in section 2.4. If we focus on the posterior convergence rate rather than the P-loss convergence rate, the prior $\pi(d_j) \propto d_j^{-\nu_0/2-1}$ is enough to establish the main results in section 3.

The zero-pattern of the Cholesky factor is related to the directed acyclic graph (Rütimann and Bühlmann, 2009). The use of the k -BC prior (2.4) implies that we approximate the true model with a directed Gaussian graphical model. Thus, our method can be applied to directed Gaussian graphical models, but applications to graphical models will not be discussed in this paper. For more details about graphical models, see Lauritzen (1996), Koller and Friedman (2009) and Rütimann and Bühlmann (2009).

2.3 Parameter Class

For a given constant $\epsilon_0 > 0$ and a decreasing function $\gamma(k) \rightarrow 0$ as $k \rightarrow \infty$, we define a class of precision matrices

$$\begin{aligned} \mathcal{U}(\epsilon_0, \gamma) = \mathcal{U}_p(\epsilon_0, \gamma) = & \left\{ \Omega = (I_p - A)^T D^{-1} (I_p - A) \in \mathcal{C}_p : \right. \\ & \left. \epsilon_0 \leq \lambda_{\min}(\Omega) \leq \lambda_{\max}(\Omega) \leq \epsilon_0^{-1}, \|A - B_k(A)\|_{\infty} \leq \gamma(k), \forall 0 < k \leq p-1 \right\}, \end{aligned} \quad (2.8)$$

2.3 Parameter Class

where \mathcal{C}_p is the class of all $p \times p$ dimensional positive definite matrices, and $A = (a_{ij})$ is a lower triangular matrix from the modified Cholesky decomposition of Ω , and $B_k(A) := (b_{ij} = a_{ij}I(|i - j| \leq k), 1 \leq i, j \leq p)$.

Thus, $\|A - B_k(A)\|_\infty \leq \gamma(k)$ is equivalent to $\max_{1 \leq i \leq p} \sum_{j < i-k} |a_{ij}| \leq \gamma(k)$.

We consider the following classes of $\gamma(k)$:

1. (polynomially decreasing) $\gamma(k) = Ck^{-\alpha}$ for some $\alpha > 0$ and $C > 0$;
2. (exponentially decreasing) $\gamma(k) = Ce^{-\beta k}$ for some $\beta > 0$ and $C > 0$;

and

3. (exact banding) for some $k_0 > 0$, $\gamma(k) = 0$ for all $k > k_0$.

Banerjee and Ghosal (2014) considered a similar parameter space for precision matrix defined by

$$\mathcal{U}^*(\epsilon_0, \gamma) = \mathcal{U}_p^*(\epsilon_0, \gamma) = \left\{ \Omega = (\omega_{ij}) \in \mathcal{C}_p : 0 < \epsilon_0 \leq \lambda_{\min}(\Omega) \leq \lambda_{\max}(\Omega) \leq \epsilon_0^{-1}, \right. \\ \left. \max_{1 \leq i \leq p} \sum_{j: |i-j| > k} |\omega_{ij}| \leq \gamma(k), \forall 0 < k \leq p-1 \right\}.$$

If we consider an exact banding $\gamma(k)$ or an exponentially decreasing $\gamma(k)$ with $\beta > \log(\epsilon_0^{-2} + 1)$, two classes $\mathcal{U}(\epsilon_0, \gamma)$ and $\mathcal{U}^*(\epsilon_0, \gamma)$ are *equivalent*, in terms of the convergence rate over them. For the polynomially decreasing $\gamma(k)$ with $\alpha > 1$, $\Omega \in \mathcal{U}(\epsilon_0, \gamma)$ does not guarantee $\Omega \in \mathcal{U}^*(\epsilon_0, \gamma)$, but still two classes are related. The following proposition describes the relation between them, and its proof is given in Supplementary material.

2.4 Bayesian Minimax Rate

Proposition 1. *Suppose γ is a decreasing function defined on positive integers. If γ is exponentially decreasing with $\gamma(k) = Ce^{-\beta k}$ with $\beta > \log(\epsilon_0^{-2} + 1)$ and $C > 0$, or exact banding for some $k_0 > 0$, then*

$$\mathcal{U}(\epsilon_0, C_1\gamma) \subseteq \mathcal{U}^*(\epsilon_0, \gamma) \subseteq \mathcal{U}(\epsilon_0, C_2\gamma),$$

and if $\gamma(k) = Ck^{-\alpha}$ with $\alpha > 1$, then

$$\mathcal{U}(\epsilon_0, \gamma) \subseteq \mathcal{U}^*(\epsilon_0, C_3\gamma'),$$

where $\gamma'(k) = Ck^{-(\alpha-1)}$, for some positive constants C_1, C_2 and C_3 not depending on p .

2.4 Bayesian Minimax Rate

Posterior convergence rate is the most commonly used measure about the asymptotic concentration of posterior around the true parameter (Ghosal et al., 2000; Ghosal and van der Vaart, 2007). The concept of the posterior convergence rate is used to justify priors, but the best possible posterior convergence rate is an elusive concept to define. Motivated by the aforementioned difficulty, a new decision theoretic framework for prior selection was suggested by Lee and Lee (2018).

Consider a prior $\pi(\Omega)$ as a decision rule and define the P-loss as

$$\mathcal{L}(\Omega_{0,n}, \pi) = \mathbb{E}^\pi(d(\Omega, \Omega_{0,n}) | \mathbf{X}_n),$$

2.4 Bayesian Minimax Rate

where $d(\Omega, \Omega')$ is a pseudometric on a set of positive definite matrices, $\Omega_{0,n}$ is the true precision matrix, and $\mathbb{E}^\pi(\cdot | \mathbf{X}_n)$ is the expectation under the posterior of Ω when the prior π and observation \mathbf{X}_n are given. The P-risk is defined as

$$\mathcal{R}(\Omega_{0,n}, \pi) = \mathbb{E}_{0n} \mathbb{E}^\pi (d(\Omega, \Omega_{0,n}) | \mathbf{X}_n), \quad (2.9)$$

where $\mathbb{E}_{0n} = \mathbb{E}_{\Omega_{0,n}}$ denotes the expectation with respect to $X_1, \dots, X_n \stackrel{iid}{\sim} N_p(0, \Omega_{0,n}^{-1})$. Let Π_n be the class of all priors on \mathcal{C}_p . Then, the Bayesian minimax rate of the posterior for the class $\mathcal{C}_p^* \subset \mathcal{C}_p$ and the space of prior distributions $\Pi_n^* \subset \Pi_n$ is naturally defined as a sequence r_n such that

$$\inf_{\pi \in \Pi_n^*} \sup_{\Omega_{0,n} \in \mathcal{C}_p^*} \mathbb{E}_{0n} \mathcal{L}(\Omega_{0,n}, \pi(\cdot | \mathbf{X}_n)) \asymp r_n.$$

If a prior π^* satisfies

$$\sup_{\Omega_{0,n} \in \mathcal{C}_p^*} \mathbb{E}_{0n} \mathcal{L}(\Omega_{0,n}, \pi^*(\cdot | \mathbf{X}_n)) \lesssim a_n,$$

then π^* is said to have a P-loss convergence rate a_n , and if a_n has the same rate with the Bayesian minimax rate, i.e. $a_n \asymp r_n$, π^* is said to achieve the Bayesian minimax rate. The new decision theoretic view of posterior analysis makes optimal properties conceptually transparent even if the class of priors and the parameter space are constrained. It also opens possibility of studying optimality properties of pseudo-posteriors such as

consensus Monte Carlo Scott et al. (2016). P-loss convergence rate is a stronger measure than posterior convergence rate, and a frequentist minimax lower bound is also a Bayesian minimax lower bound in general. See Proposition A.1 and Proposition A.2 in Lee and Lee (2018).

3. Main Results

3.1 P-loss Convergence Rate and Bayesian Minimax Lower Bound under Spectral Norm

In this subsection, we establish Bayesian minimax lower and upper bounds under the spectral norm. The P-loss convergence rate with the k -BC prior (2.4) is one of the main results of this paper. The rate obtained in Theorem 2 is slightly slower than the rate of a frequentist minimax lower bound given in Theorem 1. The proofs of theorems are given in Supplementary material.

Theorem 1. *Consider model (2.1) with $p \leq \exp(cn)$ for some constant $c > 0$. Assume $\Omega_{0,n} \in \mathcal{U}(\epsilon_0, \gamma)$, which is defined at (2.8), for given $\epsilon_0 > 0$ and a decreasing function γ .*

(i) *If there exists a constant $k_0 > 0$ such that $\gamma(k) = 0$ for all $k \geq k_0$, we have*

$$\inf_{\hat{\Omega}_n} \sup_{\Omega_{0,n} \in \mathcal{U}(\epsilon_0, \gamma)} \mathbb{E}_{0n} \|\hat{\Omega}_n - \Omega_{0,n}\| \gtrsim \left(\frac{\log p}{n} \right)^{1/2},$$

3.1 P-loss Convergence Rate and Bayesian Minimax Lower Bound under Spectral Norm¹⁶

where $\widehat{\Omega}_n$ denotes an arbitrary estimator of $\Omega_{0,n}$.

(ii) If $\gamma(k) = Ce^{-\beta k}$ for some constants $\beta > 0$ and $C > 0$, then we have

$$\inf_{\widehat{\Omega}_n} \sup_{\Omega_{0,n} \in \mathcal{U}(\epsilon_0, \gamma)} \mathbb{E}_{0n} \|\widehat{\Omega}_n - \Omega_{0,n}\| \gtrsim \min \left\{ \left(\frac{\log(n \vee p)}{n} \right)^{1/2}, \left(\frac{p}{n} \right)^{1/2} \right\}.$$

(iii) If $\gamma(k) = Ck^{-\alpha}$ for some constants $\alpha > 0$ and $C > 0$, then we have

$$\inf_{\widehat{\Omega}_n} \sup_{\Omega_{0,n} \in \mathcal{U}(\epsilon_0, \gamma)} \mathbb{E}_{0n} \|\widehat{\Omega}_n - \Omega_{0,n}\| \gtrsim \min \left\{ \left(\frac{\log p}{n} \right)^{1/2} + n^{-\alpha/(2\alpha+1)}, \left(\frac{p}{n} \right)^{1/2} \right\}.$$

The estimation of precision matrix with polynomially banded Cholesky factor under the spectral norm was studied by Bickel and Levina (2008b), but they did not consider a minimax lower bound. Verzelen (2010) obtained a minimax lower bound, but he considered the sparse Cholesky factor under the Frobenius norm.

Cai and Yuan (2016) considered the estimation of covariance operator for random variables on a lattice graph under the spectral norm. They used exponentially (and polynomially) bandable assumption for the covariance operator. In one-dimensional lattice case, interestingly the minimax lower bound in Cai and Yuan (2016) coincide with a minimax lower bound in Theorem 1 (ii). This makes sense because two classes are equivalent by Proposition 1.

Remark 3. Since a frequentist minimax lower bound is also a P-loss minimax lower bound, Theorem 1 renders a P-loss minimax lower bound. For

3.1 P-loss Convergence Rate and Bayesian Minimax Lower Bound under Spectral Norm 17

the proof of this argument, see Proposition A.2 in Lee and Lee (2018).

Remark 4. Recently, Liu and Ren (2017) obtained the minimax lower bound with respect to the spectral norm, concurrently with our work. Their lower bound is sharper than that in (iii) of Theorem 1, and they showed that it is the minimax rate. However, Liu and Ren (2017) considered only the polynomially decreasing $\gamma(k) = Ck^{-\alpha}$, while we also provided lower bounds for exponentially decreasing and exactly banded $\gamma(k)$. Furthermore, we also considered the “small p ” case, $p = o(n)$, while Liu and Ren (2017) assumed $n = O(p)$. Specifically, under conditions $\log p = O(n)$ and $n = O(p)$, they proved

$$\inf_{\hat{\Omega}_n} \sup_{\Omega_{0,n} \in \mathcal{U}(\epsilon_0, \gamma)} \mathbb{E}_{0n} \|\hat{\Omega}_n - \Omega_{0,n}\| \gtrsim \left(\frac{\log p}{n} \right)^{1/2} + n^{(-2\alpha+1)/4\alpha}, \quad (3.1)$$

where $\gamma(k) = Ck^{-\alpha}$ for some constants $\alpha > 1/2$ and $C > 0$. Under their assumptions, a lower bound in (iii) of Theorem 1 is quite close to that of in (3.1).

The P-loss convergence rate of the k -BC prior (2.4) under the spectral norm is given in the following theorem.

Theorem 2. Consider the model (2.1) and the k -BC prior (2.4) for the precision matrix $\Omega_n = (I_p - A_n)^T D_n^{-1} (I_p - A_n)$ with $M \geq 9\epsilon_0^{-1}$ and $\nu_0 = o(n)$ for a given constant $\epsilon_0 > 0$. If $k^{3/2}(k + \log(n \vee p)) = O(n)$, $k + \log p = o(n)$

3.1 P-loss Convergence Rate and Bayesian Minimax Lower Bound under Spectral Norm18

and $1 \leq k \leq p - 1$,

$$\sup_{\Omega_{0,n} \in \mathcal{U}(\epsilon_0, \gamma)} \mathbb{E}_{0n} \mathbb{E}^\pi (\|\Omega_n - \Omega_{0,n}\| \mid \mathbf{X}_n) \lesssim k^{3/4} \left[\left(\frac{k + \log(n \vee p)}{n} \right)^{1/2} + \gamma(k) \right],$$

where $\mathcal{U}(\epsilon_0, \gamma)$ is defined at (2.8) and $\sum_{m=1}^{\infty} \gamma(m) < \infty$.

Note that because we impose the k -BC prior on the precision matrix Ω_n , the posterior for Ω_n also is supported on k -banded positive definite matrices.

In the proof, we use divide and conquer strategy to deal with the P-loss convergence rate. We decompose it into small terms, which are easier to handle, i.e.,

$$\mathbb{E}_{0n} \mathbb{E}^\pi (\|\Omega_n - \Omega_{0,n}\| \mid \mathbf{X}_n) \leq \mathbb{E}_{0n} \mathbb{E}^\pi (\|\Omega_n - \widehat{\Omega}_{nk}\| \mid \mathbf{X}_n) + \mathbb{E}_{0n} \|\widehat{\Omega}_{nk} - \Omega_{0,n}\|,$$

where $\widehat{\Omega}_{nk}$ is a frequentist estimator of $\Omega_{0,n}$ that is a k -banded positive definite matrix. For the first term, we use concentration inequalities for posteriors of parameters around certain frequentist estimators. For the second term, techniques for the frequentist convergence rate can be adopted.

We summarized P-loss convergence rates and minimax lower bounds under the spectral norm for various types of γ in $\mathcal{U}(\epsilon_0, \gamma)$ at Table 1. For the second row, we assumed k_0 is fixed. The second column shows the P-loss convergence rates with optimal choices of k , which minimize the convergence rates in Theorem 2. Optimal values of k are k_0 , $(2\beta)^{-1} \log n$ and

3.2 P-loss Convergence Rate and Bayesian Minimax Lower Bound under Matrix ℓ_∞ Norm

Table 1: A summary of P-loss convergence rates and minimax lower bounds under the spectral norm for various types of γ . The second column shows the P-loss convergence rate in Theorem 2 with the optimal choice of k .

Type of γ	P-loss convergence rate	Minimax lower bound
$\gamma(k) = 0$ for $k > k_0$	$\left(\frac{\log(n \vee p)}{n}\right)^{\frac{1}{2}}$	$\left(\frac{\log p}{n}\right)^{\frac{1}{2}}$
$\gamma(k) = Ce^{-\beta k}$, $\beta > 0$	$(\log n)^{\frac{3}{4}} \left(\frac{\log(n \vee p)}{n}\right)^{\frac{1}{2}}$	$\left(\frac{\log(n \vee p)}{n}\right)^{\frac{1}{2}}$ if $p \geq \log n$
$\gamma(k) = Ck^{-\alpha}$	$\left(\frac{\log p}{n}\right)^{\frac{4\alpha-3}{8\alpha}} + n^{-\frac{4\alpha-3}{8\alpha+4}}$ if $p \geq n^{1/(2\alpha)}$, $\alpha > 1$	$\left(\frac{\log p}{n}\right)^{\frac{1}{2}} + n^{-\frac{2\alpha-1}{4\alpha}}$, $\alpha > \frac{1}{2}$

$\min\{n^{1/(2\alpha+1)}, (n/\log p)^{1/(2\alpha)}\}$ for the second, third and fourth rows, respectively. Based on Table 1, one can see that the P-loss convergence rate with optimal k coincide or quite close to the minimax lower bound for every setting. Note that the P-loss convergence rate in the fourth row is equal to the rate of the minimax lower bound up to $\min\{n^{(3\alpha-1)/[\alpha(8\alpha+4)]}, (n/\log p)^{3/(8\alpha)}\}$.

3.2 P-loss Convergence Rate and Bayesian Minimax Lower Bound under Matrix ℓ_∞ Norm

In this subsection, we establish upper and lower bounds for the Bayesian minimax rate under the matrix ℓ_∞ norm. The P-loss convergence rate obtained in Theorem 4 is slightly slower than the rate of a minimax lower bound given in Theorem 3. However, we emphasize that our convergence rate is the fastest rate for bandable precision matrices among the existing Bayesian methods. The proofs of theorems are given in Supplementary

3.2 P-loss Convergence Rate and Bayesian Minimax Lower Bound under Matrix ℓ_∞ Norm20

material.

Theorem 3. Consider the model (2.1) and let $p \leq \exp(cn)$ for some constant $c > 0$. Assume $\Omega_{0,n} \in \mathcal{U}(\epsilon_0, \gamma)$, which is defined at (2.8), for given $\epsilon_0 > 0$ and a decreasing function γ .

(i) If there exists a constant k_0 such that $\gamma(k) = 0$ for all $k \geq k_0$, we have

$$\inf_{\hat{\Omega}_n} \sup_{\Omega_{0,n} \in \mathcal{U}(\epsilon_0, \gamma)} \mathbb{E}_{0n} \|\hat{\Omega}_n - \Omega_{0,n}\|_\infty \gtrsim \left(\frac{\log p}{n} \right)^{1/2}.$$

(ii) If $\gamma(k) = Ce^{-\beta k}$ for some constants $\beta > 0$ and $C > 0$, then we have

$$\inf_{\hat{\Omega}_n} \sup_{\Omega_{0,n} \in \mathcal{U}(\epsilon_0, \gamma)} \mathbb{E}_{0n} \|\hat{\Omega}_n - \Omega_{0,n}\|_\infty \gtrsim \min \left\{ \left(\frac{\log p \log n}{n} \right)^{1/2}, \frac{p}{\sqrt{n}} \right\}.$$

(iii) If $\gamma(k) = Ck^{-\alpha}$ for some constants $\alpha > 0$ and $C > 0$, then we have

$$\inf_{\hat{\Omega}_n} \sup_{\Omega_{0,n} \in \mathcal{U}(\epsilon_0, \gamma)} \mathbb{E}_{0n} \|\hat{\Omega}_n - \Omega_{0,n}\|_\infty \gtrsim \min \left\{ \left(\frac{\log p}{n} \right)^{\alpha/(2\alpha+1)} + n^{-\alpha/(2\alpha+2)}, \frac{p}{\sqrt{n}} \right\}.$$

Theorem 4. Consider the model (2.1) and the k -BC prior (2.4) for the precision matrix $\Omega_n = (I_p - A_n)^T D_n^{-1} (I_p - A_n)$ with $M \geq 9\epsilon_0^{-1}$ and $\nu_0 = o(n)$ for a given constant $\epsilon_0 > 0$. If $k(k + \log(n \vee p)) = O(n)$, $k + \log p = o(n)$ and $1 \leq k \leq p - 1$,

$$\sup_{\Omega_{0,n} \in \mathcal{U}(\epsilon_0, \gamma)} \mathbb{E}_{0n} \mathbb{E}^\pi (\|\Omega_n - \Omega_{0,n}\|_\infty \mid \mathbf{X}_n) \lesssim k \left[\left(\frac{k + \log(n \vee p)}{n} \right)^{1/2} + \gamma(k) \right],$$

where $\mathcal{U}(\epsilon_0, \gamma)$ is defined at (2.8) and $\sum_{m=1}^{\infty} \gamma(m) < \infty$.

3.2 P-loss Convergence Rate and Bayesian Minimax Lower Bound under Matrix ℓ_∞ Norm

Table 2: A summary of P-loss convergence rates and minimax lower bounds under the matrix ℓ_∞ norm for various types of γ . The second column shows the P-loss convergence rate in Theorem 4 with the optimal choice of k .

Type of γ	P-loss convergence rate	Minimax lower bound
$\gamma(k) = 0$ for $k > k_0$	$\left(\frac{\log(n \vee p)}{n}\right)^{\frac{1}{2}}$	$\left(\frac{\log p}{n}\right)^{\frac{1}{2}}$
$\gamma(k) = Ce^{-\beta k}$	$\log n \left(\frac{\log(n \vee p)}{n}\right)^{\frac{1}{2}}$	$\left(\frac{\log p \log n}{n}\right)^{\frac{1}{2}}$ if $p \geq (\log n \log p)^{1/2}$
$\gamma(k) = Ck^{-\alpha}$	$\left(\frac{\log p}{n}\right)^{\frac{\alpha-1}{2\alpha}} + n^{-\frac{\alpha-1}{2\alpha+1}}$ if $p \geq n^{1/(2\alpha+2)}, \alpha > 1$	$\left(\frac{\log p}{n}\right)^{\frac{\alpha}{2\alpha+1}} + n^{-\frac{\alpha}{2\alpha+2}}, \alpha > 0$

We summarized P-loss convergence rates and minimax lower bounds under the matrix ℓ_∞ norm for various types of γ in $\mathcal{U}(\epsilon_0, \gamma)$ at Table 2. As in Table 1, we assumed k_0 is fixed and represented the P-loss convergence rates with optimal choices of k , which minimize the convergence rates in Theorem 4. Optimal values of k are the same with those in section 3.1. Based on Table 2, one can see that the P-loss convergence rate with optimal k coincide or quite close to a minimax lower bound for every setting.

Remark 5. The P-loss convergence rate in Theorem 4 is sharper than the posterior convergence rate of Banerjee and Ghosal (2014). If we consider an exponentially decreasing or exact banding $\gamma(k)$, then the parameter spaces in two papers are equivalent by Proposition 1. In that cases, the convergence rate obtained in Theorem 4 is equal or faster than that in Banerjee and Ghosal (2014). When $\gamma(k) = Ck^{-\alpha}$, we have $\mathcal{U}(\epsilon_0, \gamma) \subseteq \mathcal{U}^*(\epsilon_0, \gamma')$, where $\gamma'(k) = C'k^{-(\alpha-1)}$ for some constant $C' > 0$ by Proposition 1. Thus, the

3.3 Frequentist Convergence Rates and Posterior Convergence Rates 22

rate obtained in Theorem 4 can be directly compared with that in Banerjee and Ghosal (2014) under the parameter class $\mathcal{U}(\epsilon_0, \gamma) \cap \mathcal{U}^*(\epsilon_0, \gamma')$. With the optimal choice of k for each result, the former is

$$\left(\frac{\log p}{n}\right)^{\frac{\alpha-1}{2\alpha}} + n^{-\frac{\alpha-1}{2\alpha+1}}$$

and the latter is $(\log p/n)^{(2\alpha-5)/(4\alpha)}$. The rate obtained in Theorem 4 is faster than that in Banerjee and Ghosal (2014) by factors $n^{(4\alpha+5)/[4\alpha(2\alpha+1)]}$ and $(n/\log p)^{3/(4\alpha)}$ when $n^{1/(2\alpha+2)} \leq p \leq \exp(n^{1/(2\alpha+1)})$ and $p \geq \exp(n^{1/(2\alpha+1)})$, respectively.

3.3 Frequentist Convergence Rates and Posterior Convergence Rates

In this subsection, we obtain the frequentist convergence rate and the traditional posterior convergence rate of the k -BC prior (2.4). For the frequentist convergence rate, we propose a plug-in estimator,

$$\widehat{\Omega}_{nk}^{LL} = (I_p - \mathbb{E}^\pi(A_n | \mathbf{X}_n))^T \mathbb{E}^{\tilde{\pi}}(D_n^{-1} | \mathbf{X}_n) (I_p - \mathbb{E}^\pi(A_n | \mathbf{X}_n)), \quad (3.2)$$

where $\mathbb{E}^{\tilde{\pi}}(\cdot | \mathbf{X}_n)$ are posterior means using the non-truncated posteriors,

$$\tilde{\pi}(d_j | \mathbf{X}_n) = IG\left(d_j \mid \frac{n_j}{2}, \frac{n}{2} \widehat{d}_{jk}\right), \quad j = 1, \dots, p.$$

The plug-in estimator $\widehat{\Omega}_{nk}^{LL}$ is more convenient than the posterior mean $\mathbb{E}^\pi(\Omega_n | \mathbf{X}_n)$ in practice because of its simple form. Note that $\mathbb{E}^\pi(a_j^{(k)} |$

3.3 Frequentist Convergence Rates and Posterior Convergence Rates²³

$d_j, \mathbf{X}_n) = \widehat{a}_j^{(k)}$ and $\mathbb{E}^{\tilde{\pi}}(d_j^{-1} \mid \mathbf{X}_n) = n_j \widehat{d}_{jk}^{-1}/n$. As a justification for the use of the non-truncated posterior mean, in Corollary 1, we show that $\widehat{\Omega}_{nk}^{LL}$ achieves the same rate with the P-loss convergence rate. The proof of Corollary 1 is given in Supplementary material.

According to Proposition A.1 of Lee and Lee (2018), a P-loss convergence rate is a posterior convergence rate. Thus, Corollary 2 follows from Proposition A.1 of Lee and Lee (2018), which means that the rates obtained in Theorem 2 and Theorem 4 in this paper are also posterior convergence rates.

Corollary 1. *Consider the model (2.1) and $\mathcal{U}(\epsilon_0, \gamma)$ defined at (2.8), and assume $k + \log p = o(n)$, $\sum_{m=1}^{\infty} \gamma(m) < \infty$, $\nu_0 = o(n)$ and $1 \leq k \leq p$. If $k^{3/2}(k + \log(n \vee p)) = O(n)$,*

$$\sup_{\Omega_{0,n} \in \mathcal{U}(\epsilon_0, \gamma)} \mathbb{E}_{0n} \|\widehat{\Omega}_{nk}^{LL} - \Omega_{0,n}\| \lesssim k^{3/4} \left[\left(\frac{k + \log(n \vee p)}{n} \right)^{1/2} + \gamma(k) \right].$$

If $k(k + \log(n \vee p)) = O(n)$,

$$\sup_{\Omega_{0,n} \in \mathcal{U}(\epsilon_0, \gamma)} \mathbb{E}_{0n} \|\widehat{\Omega}_{nk}^{LL} - \Omega_{0,n}\|_{\infty} \lesssim k \left[\left(\frac{k + \log(n \vee p)}{n} \right)^{1/2} + \gamma(k) \right].$$

Corollary 2. *Consider the model (2.1), $\mathcal{U}(\epsilon_0, \gamma)$ defined at (2.8) and the k -BC prior (2.4) with $M \geq 9\epsilon_0^{-1}$ and $\nu_0 = o(n)$. Assume $k + \log p = o(n)$, $\sum_{m=1}^{\infty} \gamma(m) < \infty$ and $1 \leq k \leq p$. If $k^{3/2}(k + \log(n \vee p)) = O(n)$ and*

$\epsilon_n = k^{3/4} [(k + \log(n \vee p))/n]^{1/2} + \gamma(k)$, then for any $M_n \rightarrow \infty$ as $n \rightarrow \infty$,

$$\sup_{\Omega_{0,n} \in \mathcal{U}(\epsilon_0, \gamma)} \mathbb{E}_{0n} \left[\pi(\|\Omega_n - \Omega_{0,n}\| \geq M_n \epsilon_n \mid \mathbf{X}_n) \right] \rightarrow 0.$$

If $k(k + \log(n \vee p)) = O(n)$ and $\epsilon_n^* = k [((k + \log(n \vee p))/n)^{1/2} + \gamma(k)]$,

then for any $M_n \rightarrow \infty$ as $n \rightarrow \infty$,

$$\sup_{\Omega_{0,n} \in \mathcal{U}(\epsilon_0, \gamma)} \mathbb{E}_{0n} \left[\pi(\|\Omega_n - \Omega_{0,n}\|_\infty \geq M_n \epsilon_n^* \mid \mathbf{X}_n) \right] \rightarrow 0.$$

4. Choice of the Bandwidth k

In this section, we suggest using the posterior mode of k as a practical choice of the bandwidth k . Using Theorem 2 and Theorem 4, one can calculate the optimal *rate* of the bandwidth k minimizing the P-loss convergence rate, when the rate of $\gamma(k)$ is given. However, it does not provide a proper choice of k in practice because $\gamma(k)$ is unknown.

Let $\pi(k)$ be a prior distribution for the bandwidth k and $f(\mathbf{X}_n \mid A_n, D_n, k)$ be the likelihood function based on the observation \mathbf{X}_n . In section 5, the prior distribution of k is set by $\pi(k) \propto \exp(-k^4)$ as in Banerjee and Ghosal

(2014). The marginal posterior for k is easily derived as

$$\begin{aligned}
 \pi(k | \mathbf{X}_n) &\propto \pi(k) \int \int f(\mathbf{X}_n | A_n, D_n, k) \pi(A_n, D_n | k) dA_n dD_n \\
 &\propto \pi(k) \prod_{j=2}^p \det(X_{\cdot, (j-k):(j-1)}^T X_{\cdot, (j-k):(j-1)} / (2\pi))^{-1/2} \Gamma\left(\frac{n_j}{2}\right) \left(\frac{n}{2} \hat{d}_{jk}\right)^{-n_j/2} \\
 &\times \prod_{j=1}^p F_{IG}\left(M \mid n_j/2, n \hat{d}_{jk}/2\right)
 \end{aligned} \tag{4.3}$$

by routine calculations, where $\pi(A_n, D_n | k)$ denotes the k -BC prior (2.4), $\det(\cdot)$ is the determinant function, $\Gamma(\cdot)$ is the gamma function, and $F_{IG}(M | a, b)$ is a cumulative distribution function of $IG(a, b)$. Since the marginal posterior (4.3) has a simple analytic form, the posterior mode, say \hat{k} , can be easily obtained. The performance of \hat{k} is described through comparisons with other approaches in the next section.

Note that the Cholesky-based Bayes estimator $\hat{\Omega}_{nk}^{LL}$ is similar to the banded estimator (Bickel and Levina, 2008b), $\hat{\Omega}_{nk}^{BL}$. The major difference between two estimators is the choice of the bandwidth parameter k . Bickel and Levina (2008b) proposed a resampling scheme to estimate the oracle k , which minimizes

$$R(k) = \mathbb{E}_{0n} \|\hat{\Omega}_{nk}^{BL} - \Omega_{0,n}\|_1. \tag{4.4}$$

To approximate the risk in (4.4), they randomly divided n observations into two groups of sizes $n_1 = n/3$ and $n_2 = n - n_1$. They calculated the

banded estimator based on the first group, say $\widehat{\Omega}_{1,nk}^{BL}$, and used it for $\widehat{\Omega}_{nk}^{BL}$ in (4.4). The second group is used to approximate $\Omega_{0,n}$ in (4.4), but Bickel and Levina (2008b) did not suggest which estimator we would use. Since the sample precision matrix is computationally unstable for large p , we used the banded estimator with $K = 20$ based on the second group, say $\widehat{\Omega}_{2,nK}^{BL,(t)}$, in the simulation study. In the same way, t th random split gives $\widehat{\Omega}_{1,nk}^{BL,(t)}$ and $\widehat{\Omega}_{2,nk}^{BL,(t)}$ for $t = 1, \dots, T$. Finally, the risk (4.4) is approximated by

$$\widehat{R}(k) = \frac{1}{T} \sum_{t=1}^T \|\widehat{\Omega}_{1,nk}^{BL,(t)} - \widehat{\Omega}_{2,nK}^{BL,(t)}\|_1, \quad (4.5)$$

and the bandwidth k was selected as $\hat{k}^{BL} = \operatorname{argmin}_{0 \leq k \leq K} \widehat{R}(k)$, where $K = 20$. \hat{k}^{BL} does not need to minimize the ℓ_1 norm risk in practice, because its consistency is not guaranteed.

5. Simulation Study

We investigated the performance of the proposed Bayes estimator $\widehat{\Omega}_{nk}^{LL}$, defined in (3.2), and the posterior mode \hat{k} . The performances of the Bayes estimator based on the G -Wishart prior $\widehat{\Omega}_{nk}^{BG}$ (Banerjee and Ghosal, 2014) and the banded estimator $\widehat{\Omega}_{nk}^{BL}$ (Bickel and Levina, 2008b) were compared in various scenarios. For the proposed estimator $\widehat{\Omega}_{nk}^{LL}$, we used $\nu_0 = 2$ throughout this section.

Banerjee and Ghosal (2014) proposed two Bayes estimators corresponding to the Stein's loss and the squared-error loss, respectively. We checked the performances of two Bayes estimators, say $\widehat{\Omega}_{nk}^{BG1}$ and $\widehat{\Omega}_{nk}^{BG2}$, with $\delta = 3$. For these estimators, the bandwidth k was chosen by the posterior mode in Banerjee and Ghosal (2014), \hat{k}^{BG} .

For the banded Cholesky-based estimator proposed by (Bickel and Levina, 2008b), we tried two different bandwidth estimators, \hat{k}^{BL} and \hat{k} , to compare their performances.

The spectral norm, matrix ℓ_∞ norm and Frobenius norm were used as the loss functions. The sample sizes $n = 100, 200$ and 500 and the dimensions $p = 100, 200$ and 500 were investigated. For each settings, the values of the loss function,

$$\|\widehat{\Omega}_{nk}^{(s)} - \Omega_{0,n}\|, \quad s = 1, \dots, 100, \quad (5.6)$$

were calculated with 100 simulated data for each methods $\widehat{\Omega}_{nk}$ and loss functions $\|\cdot\|$, where $\Omega_{0,n}$ denotes the true precision matrix. The mean and standard deviation of (5.6) were used as summary statistics. We considered the following true precision matrices.

Example 1. (*AR*(1) process) Assume the true covariance matrix $\Sigma_{0,n} =$

$(\sigma_{0,ij})$ is given by

$$\sigma_{0,ij} = \rho^{|i-j|}, \quad 1 \leq i, j \leq p$$

with $\rho = 0.3$. Then the true precision matrix is a banded matrix with $AR(1)$ process structure.

Example 2. ($AR(4)$ process) Assume the true precision matrix $\Omega_{0,n} = (\omega_{0,ij})$ is given by

$$\begin{aligned} \omega_{0,ij} = & I(|i-j|=0) + 0.4 \cdot I(|i-j|=1) + 0.2 \cdot I(|i-j|=2) \\ & + 0.2 \cdot I(|i-j|=3) + 0.1 \cdot I(|i-j|=4). \end{aligned}$$

Thus, the true precision matrix is a banded matrix with the $AR(4)$ process structure. Furthermore, it is always positive definite because of the diagonally dominant property.

Example 3. (Long-range dependence) The last example deals with the situation where the true precision matrix is not a bandable matrix in $\mathcal{U}(\epsilon_0, \gamma)$. Consider a fractional Gaussian noise model and the true covariance matrix

$\Sigma_{0,n} = (\sigma_{0,ij})$ is given by

$$\sigma_{0,ij} = \frac{1}{2} (||i-j|+1|^{2H} - 2|i-j|^{2H} + ||i-j|-1|^{2H}), \quad 1 \leq i, j \leq p$$

with $H \in [0.5, 1]$. The Hurst parameter H indicates the dependency of the process. $H = 0.5$ implies the white noise, while H near 1 means the

long-range dependence. We chose $H = 0.7$. In this case, the true precision matrix does not belong to the bandable class.

Table 3–5 show the simulation results for the above three examples, and Figure 1 shows the performance of each estimator when the true precision matrix is $AR(4)$ process and $(n, p) = (500, 500)$. We omitted the estimator $\hat{\Omega}_{nk}^{BG2}$ because its performance is quite similar to that of $\hat{\Omega}_{nk}^{BG1}$ throughout the all scenarios, where BG in Table 3–5 and Figure 1 represents $\hat{\Omega}_{nk}^{BG1}$.

We also reported the summary statistics for estimated bandwidths, \hat{k} ,

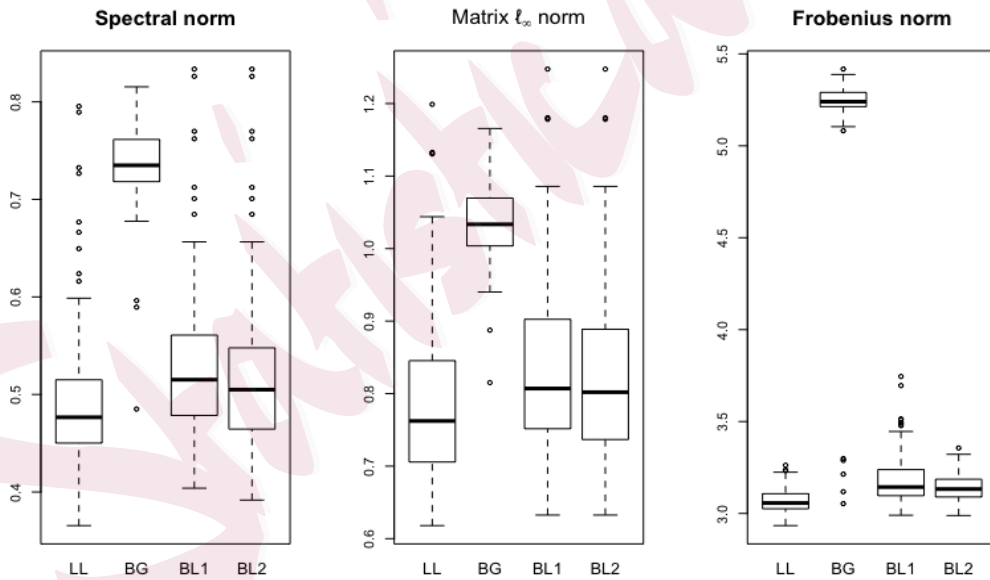


Figure 1: The average errors for $AR(4)$ process structure precision matrix under the spectral norm, matrix ℓ_∞ norm and Frobenius norm. The sample size n and the dimensionality p are 500.

Table 3: Simulation results for $AR(1)$ model. For each n and p , the mean and standard deviation (in parenthesis) of three loss functions (the spectral norm, matrix ℓ_∞ norm and Frobenius norm) were calculated. $BL1$ and $BL2$ columns in tables show the results for banded estimators with the bandwidth \hat{k}^{BL} and \hat{k} , respectively.

		LL	BG	BL1	BL2	
$p = 100$	$\ \cdot\ $	0.720 (0.139)	0.759 (0.141)	1.217 (0.391)	0.786 (0.146)	
	$\ \cdot\ _\infty$	0.913 (0.176)	0.957 (0.177)	1.905 (0.813)	0.989 (0.184)	
	$\ \cdot\ _F$	2.382 (0.171)	2.447 (0.187)	3.837 (1.067)	2.503 (0.196)	
$n = 100$	$p = 200$	$\ \cdot\ $	0.802 (0.140)	0.842 (0.140)	1.294 (0.353)	0.873 (0.145)
	$\ \cdot\ _\infty$	1.025 (0.180)	1.071 (0.180)	2.044 (0.716)	1.108 (0.186)	
	$\ \cdot\ _F$	3.395 (0.165)	3.487 (0.179)	5.471 (0.322)	3.567 (0.188)	
$p = 500$	$\ \cdot\ $	0.910 (0.147)	0.951 (0.146)	1.504 (0.417)	0.985 (0.152)	
	$\ \cdot\ _\infty$	1.151 (0.181)	1.196 (0.181)	2.412 (0.928)	1.239 (0.188)	
	$\ \cdot\ _F$	5.377 (0.172)	5.521 (0.186)	9.070 (2.353)	5.647 (0.353)	
$p = 100$	$\ \cdot\ $	0.482 (0.090)	0.498 (0.094)	0.585 (0.165)	0.507 (0.096)	
	$\ \cdot\ _\infty$	0.619 (0.117)	0.636 (0.121)	0.815 (0.315)	0.646 (0.124)	
	$\ \cdot\ _F$	1.673 (0.110)	1.696 (0.116)	1.991 (0.442)	1.714 (0.119)	
$n = 200$	$p = 200$	$\ \cdot\ $	0.537 (0.098)	0.556 (0.100)	0.644 (0.154)	0.567 (0.102)
	$\ \cdot\ _\infty$	0.685 (0.127)	0.706 (0.130)	0.896 (0.277)	0.718 (0.133)	
	$\ \cdot\ _F$	2.374 (0.113)	2.406 (0.121)	2.851 (0.544)	2.432 (0.124)	
$p = 500$	$\ \cdot\ $	0.594 (0.124)	0.615 (0.080)	0.747 (0.156)	0.626 (0.082)	
	$\ \cdot\ _\infty$	0.755 (0.108)	0.777 (0.109)	1.054 (0.326)	0.792 (0.111)	
	$\ \cdot\ _F$	3.762 (0.104)	3.813 (0.111)	4.692 (0.866)	3.855 (0.114)	
$p = 100$	$\ \cdot\ $	0.287 (0.045)	0.292 (0.046)	0.309 (0.055)	0.295 (0.047)	
	$\ \cdot\ _\infty$	0.368 (0.060)	0.373 (0.063)	0.404 (0.084)	0.376 (0.064)	
	$\ \cdot\ _F$	1.053 (0.065)	1.060 (0.067)	1.110 (0.110)	1.064 (0.067)	
$n = 500$	$p = 200$	$\ \cdot\ $	0.314 (0.045)	0.321 (0.046)	0.340 (0.065)	0.324 (0.047)
	$\ \cdot\ _\infty$	0.405 (0.059)	0.412 (0.061)	0.445 (0.101)	0.415 (0.062)	
	$\ \cdot\ _F$	1.489 (0.073)	1.497 (0.074)	1.565 (0.172)	1.503 (0.074)	
$p = 500$	$\ \cdot\ $	0.340 (0.042)	0.347 (0.042)	0.359 (0.051)	0.350 (0.043)	
	$\ \cdot\ _\infty$	0.436 (0.053)	0.444 (0.053)	0.465 (0.078)	0.448 (0.053)	
	$\ \cdot\ _F$	2.352 (0.069)	2.365 (0.070)	2.433 (0.188)	2.375 (0.071)	

Table 4: Simulation results for $AR(4)$ model. For each n and p , the mean and standard deviation (in parenthesis) of three loss functions (the spectral norm, matrix ℓ_∞ norm and Frobenius norm) were calculated. $BL1$ and $BL2$ columns in tables show the results for banded estimators with the bandwidth \hat{k}^{BL} and \hat{k} , respectively.

		LL	BG	BL1	BL2
$p = 100$	$\ \cdot\ $	1.510 (0.040)	1.475 (0.041)	1.481 (0.340)	1.473 (0.041)
	$\ \cdot\ _\infty$	1.854 (0.058)	1.826 (0.061)	2.446 (0.607)	1.827 (0.063)
	$\ \cdot\ _F$	5.130 (0.070)	5.050 (0.065)	4.189 (0.620)	5.046 (0.065)
$n = 100$ $p = 200$	$\ \cdot\ $	1.541 (0.034)	1.506 (0.035)	1.668 (0.395)	1.504 (0.035)
	$\ \cdot\ _\infty$	1.899 (0.065)	1.873 (0.069)	2.873 (0.678)	1.874 (0.071)
	$\ \cdot\ _F$	7.312 (0.072)	7.196 (0.068)	6.015 (0.840)	7.191 (0.068)
$p = 500$	$\ \cdot\ $	1.564 (0.029)	1.530 (0.030)	1.884 (0.368)	1.528 (0.030)
	$\ \cdot\ _\infty$	1.938 (0.052)	1.913 (0.056)	3.061 (0.654)	1.915 (0.057)
	$\ \cdot\ _F$	11.610 (0.076)	11.426 (0.072)	9.620 (1.288)	11.417 (0.072)
$p = 100$	$\ \cdot\ $	1.313 (0.314)	1.461 (0.027)	0.843 (0.168)	1.288 (0.325)
	$\ \cdot\ _\infty$	1.616 (0.273)	1.734 (0.050)	1.366 (0.284)	1.596 (0.280)
	$\ \cdot\ _F$	4.477 (0.980)	4.949 (0.049)	2.513 (0.260)	4.431 (0.972)
$n = 200$ $p = 200$	$\ \cdot\ $	0.972 (0.289)	1.482 (0.027)	0.482 (0.171)	0.934 (0.299)
	$\ \cdot\ _\infty$	1.343 (0.245)	1.759 (0.043)	1.457 (0.280)	1.319 (0.249)
	$\ \cdot\ _F$	4.574 (1.357)	7.047 (0.054)	3.528 (0.336)	4.502 (1.356)
$p = 500$	$\ \cdot\ $	0.871 (0.052)	1.499 (0.023)	1.015 (0.169)	0.840 (0.059)
	$\ \cdot\ _\infty$	1.300 (0.097)	1.800 (0.041)	1.643 (0.303)	1.291 (0.117)
	$\ \cdot\ _F$	6.083 (0.345)	11.200 (0.058)	5.686 (0.554)	6.001 (0.226)
$p = 100$	$\ \cdot\ $	0.501 (0.139)	1.052 (0.395)	0.450 (0.084)	0.513 (0.122)
	$\ \cdot\ _\infty$	0.767 (0.151)	1.281 (0.355)	0.733 (0.144)	0.784 (0.137)
	$\ \cdot\ _F$	1.663 (0.444)	3.573 (1.324)	1.439 (0.118)	1.676 (0.411)
$n = 500$ $p = 200$	$\ \cdot\ $	0.447 (0.063)	0.807 (0.255)	0.481 (0.067)	0.473 (0.067)
	$\ \cdot\ _\infty$	0.722 (0.080)	1.083 (0.229)	0.768 (0.094)	0.754 (0.088)
	$\ \cdot\ _F$	1.939 (0.068)	3.764 (1.245)	2.010 (0.107)	1.985 (0.075)
$p = 500$	$\ \cdot\ $	0.493 (0.081)	0.737 (0.044)	0.530 (0.084)	0.522 (0.085)
	$\ \cdot\ _\infty$	0.784 (0.111)	1.036 (0.056)	0.835 (0.117)	0.820 (0.116)
	$\ \cdot\ _F$	3.069 (0.067)	5.151 (0.456)	3.189 (0.141)	3.139 (0.076)

Table 5: Simulation results for fractional Gaussian noise model. For each n and p , the mean and standard deviation (in parenthesis) of three loss functions (the spectral norm, matrix ℓ_∞ norm and Frobenius norm) were calculated. *BL1* and *BL2* columns in tables show the results for banded estimators with the bandwidth \hat{k}^{BL} and \hat{k} , respectively.

		LL	BG	BL1	BL2	
$n = 100$	$p = 100$	$\ \cdot\ $	0.837 (0.149)	0.880 (0.149)	1.232 (0.357)	0.911 (0.154)
		$\ \cdot\ _\infty$	1.588 (0.194)	1.636 (0.193)	2.284 (0.698)	1.676 (0.200)
		$\ \cdot\ _F$	2.879 (0.194)	2.955 (0.211)	3.980 (0.908)	3.030 (0.222)
	$p = 200$	$\ \cdot\ $	0.931 (0.147)	0.973 (0.146)	1.326 (0.335)	1.008 (0.152)
		$\ \cdot\ _\infty$	1.752 (0.188)	1.800 (0.187)	2.495 (0.654)	1.843 (0.194)
		$\ \cdot\ _F$	4.100 (0.178)	4.208 (0.194)	5.806 (1.236)	4.315 (0.204)
	$p = 500$	$\ \cdot\ $	1.043 (0.156)	1.085 (0.155)	1.493 (0.348)	1.124 (0.161)
		$\ \cdot\ _\infty$	1.929 (0.196)	1.976 (0.194)	2.800 (0.740)	2.025 (0.202)
		$\ \cdot\ _F$	6.478 (0.185)	6.648 (0.202)	9.321 (0.945)	6.817 (0.212)
$n = 200$	$p = 100$	$\ \cdot\ $	0.601 (0.096)	0.622 (0.096)	0.659 (0.126)	0.634 (0.098)
		$\ \cdot\ _\infty$	1.269 (0.137)	1.293 (0.138)	1.360 (0.217)	1.307 (0.140)
		$\ \cdot\ _F$	2.287 (0.123)	2.318 (0.131)	2.435 (0.278)	2.347 (0.134)
	$p = 200$	$\ \cdot\ $	0.665 (0.111)	0.687 (0.111)	0.719 (0.116)	0.699 (0.113)
		$\ \cdot\ _\infty$	1.400 (0.148)	1.424 (0.148)	1.484 (0.175)	1.440 (0.150)
		$\ \cdot\ _F$	3.244 (0.131)	3.289 (0.139)	3.465 (0.289)	3.330 (0.143)
	$p = 500$	$\ \cdot\ $	0.733 (0.092)	0.755 (0.092)	0.801 (0.104)	0.769 (0.094)
		$\ \cdot\ _\infty$	1.526 (0.127)	1.551 (0.127)	1.646 (0.181)	1.568 (0.129)
		$\ \cdot\ _F$	5.141 (0.117)	5.212 (0.124)	5.547 (0.464)	5.277 (0.128)
$n = 500$	$p = 100$	$\ \cdot\ $	0.406 (0.047)	0.434 (0.043)	0.436 (0.046)	0.420 (0.049)
		$\ \cdot\ _\infty$	1.004 (0.076)	1.004 (0.073)	1.046 (0.074)	1.020 (0.077)
		$\ \cdot\ _F$	1.722 (0.064)	1.875 (0.066)	1.869 (0.084)	1.742 (0.066)
	$p = 200$	$\ \cdot\ $	0.433 (0.045)	0.467 (0.044)	0.468 (0.046)	0.448 (0.046)
		$\ \cdot\ _\infty$	1.086 (0.073)	1.128 (0.073)	1.130 (0.074)	1.105 (0.074)
		$\ \cdot\ _F$	2.433 (0.063)	2.649 (0.065)	2.647 (0.085)	2.460 (0.065)
	$p = 500$	$\ \cdot\ $	0.461 (0.043)	0.495 (0.039)	0.498 (0.040)	0.476 (0.044)
		$\ \cdot\ _\infty$	1.164 (0.073)	1.203 (0.062)	1.209 (0.061)	1.183 (0.074)
		$\ \cdot\ _F$	3.856 (0.062)	4.189 (0.071)	4.202 (0.085)	3.900 (0.064)

Table 6: The mean and standard deviation (in parenthesis) of estimated values of bandwidth for $AR(1)$ model ($k_0 = 1$) in Example 1.

		\hat{k}	\hat{k}^{BG}	\hat{k}^{BL}
$n = 100$	$p = 100$	1.000 (0.000)	1.000 (0.000)	3.060 (1.638)
	$p = 200$	1.000 (0.000)	1.000 (0.000)	3.080 (1.454)
	$p = 500$	1.000 (0.000)	1.000 (0.000)	3.360 (1.667)
$n = 200$	$p = 100$	1.000 (0.000)	1.000 (0.000)	1.650 (0.999)
	$p = 200$	1.000 (0.000)	1.000 (0.000)	1.700 (0.882)
	$p = 500$	1.000 (0.000)	1.000 (0.000)	1.890 (0.952)
$n = 500$	$p = 100$	1.000 (0.000)	1.000 (0.000)	1.170 (0.377)
	$p = 200$	1.000 (0.000)	1.000 (0.000)	1.170 (0.403)
	$p = 500$	1.000 (0.000)	1.000 (0.000)	1.100 (0.333)

\hat{k}^{BG} and \hat{k}^{BL} , for $AR(1)$ and $AR(4)$ models in Table 6 and Table 7, respectively.

There are two remarks on the simulation results. First, it seems that the proposed Bayes estimator \hat{k} is practically comparable or better than the method of Banerjee and Ghosal (2014). Since theoretical results in this paper and in Banerjee and Ghosal (2014) are based on the optimal choice of k , which depends on unknown parameters, the practical performances using the posterior modes \hat{k} are of independent interest. Based on our simulation, the performance of $\hat{\Omega}_{nk}^{LL}$ is generally better than $\hat{\Omega}_{nk}^{BG1}$. Furthermore, based on Tables 6 and 7, \hat{k}^{BG} tended to underestimate the true bandwidth, and \hat{k} outperformed to \hat{k}^{BG} . Second, our selection scheme for k is comparable to

Table 7: The mean and standard deviation (in parenthesis) of estimated values of bandwidth for $AR(4)$ model ($k_0 = 4$) in Example 2.

		\hat{k}	\hat{k}^{BG}	\hat{k}^{BL}
$n = 100$	$p = 100$	1.000 (0.000)	1.000 (0.000)	5.130 (1.060)
	$p = 200$	1.000 (0.000)	1.000 (0.000)	5.170 (1.074)
	$p = 500$	1.000 (0.000)	1.000 (0.000)	5.240 (1.074)
$n = 200$	$p = 100$	1.440 (0.833)	1.000 (0.000)	4.570 (0.686)
	$p = 200$	2.560 (0.833)	1.000 (0.676)	4.530 (0.717)
	$p = 500$	3.090 (0.288)	1.000 (0.000)	4.660 (0.794)
$n = 500$	$p = 100$	3.700 (0.461)	2.000 (1.005)	4.240 (0.571)
	$p = 200$	4.000 (0.000)	2.740 (0.676)	4.110 (0.314)
	$p = 500$	4.000 (0.000)	3.050 (0.219)	4.140 (0.377)

that of Bickel and Levina (2008b), but the comparison is not straightforward because of different aspects between the two. The $BL1$ and $BL2$ columns in Tables 3–5 show the results for banded estimators of Bickel and Levina (2008b) with k chosen by \hat{k}^{BL} and \hat{k} , respectively. Based on Tables 3 and 5, the performance of $BL2$ is better than that of $BL1$, but for the second scenario (Table 4), it is hard to say which one is better than another. If we focus on Tables 6 and 7, one can see that \hat{k}^{BL} seems to overestimate the true bandwidth, while \hat{k} underestimates the true bandwidth. However, when the sample size n is large ($n = 500$), \hat{k} estimates the true bandwidth quite well, while \hat{k}^{BL} still overestimates with relatively larger variance than that of \hat{k} .

6. Discussion

We suggested the k -BC prior (2.4) for bandable precision matrices via the modified Cholesky decomposition. The P-loss convergence rates for precision matrices under the spectral norm and matrix ℓ_∞ norm were established. Although the P-loss convergence rates are slightly slower than rate of Bayesian minimax lower bounds, the proposed approach attains faster posterior convergence rate than those of the other existing Bayesian methods. Simulation study supported that its practical performance is comparable or better than those of other competitive approaches.

There are a few possible extensions of this paper related to the bandwidth k . Firstly, theoretical results in this paper depend on the unknown parameter of $\gamma(k)$. To choose the optimal k , one should know about the rate of $\gamma(k)$. Thus, developing an adaptive procedure, which simultaneously attains a reasonable convergence rate regardless of $\gamma(k)$, is one of the possible extension. Secondly, the theoretical property of the posterior mode \hat{k} is unexplored. A theoretical result similar to the Theorem 4 in Bickel and Levina (2008a) can be investigated.

Supplementary Materials

Supplementary material includes the proofs for main results and other

auxiliary results.

References

- Banerjee, S. and S. Ghosal (2014). Posterior convergence rates for estimating large precision matrices using graphical models. *Electronic Journal of Statistics* 8(2), 2111–2137.
- Banerjee, S. and S. Ghosal (2015). Bayesian structure learning in graphical models. *Journal of Multivariate Analysis* 136, 147–162.
- Bickel, P. J. and E. Levina (2008a). Covariance regularization by thresholding. *The Annals of Statistics* 36(6), 2577–2604.
- Bickel, P. J. and E. Levina (2008b). Regularized estimation of large covariance matrices. *The Annals of Statistics* 36(1), 199–227.
- Cai, T. T., T. Liang, and H. H. Zhou (2015). Law of log determinant of sample covariance matrix and optimal estimation of differential entropy for high-dimensional gaussian distributions. *Journal of Multivariate Analysis* 137, 161–172.
- Cai, T. T., W. Liu, and H. H. Zhou (2016). Estimating sparse precision matrix: Optimal rates of convergence and adaptive estimation. *The Annals of Statistics* 44(2), 455–488.
- Cai, T. T., Z. Ma, and Y. Wu (2015). Optimal estimation and rank detection for sparse spiked covariance matrices. *Probability theory and related fields* 161(3-4), 781–815.
- Cai, T. T., Z. Ren, and H. H. Zhou (2016). Estimating structured high-dimensional covariance and precision matrices: Optimal rates and adaptive estimation. *Electronic Journal of*

REFERENCES37

- Statistics* 10(1), 1–59.
- Cai, T. T. and M. Yuan (2016). Minimax and adaptive estimation of covariance operator for random variables observed on a lattice graph. *Journal of the American Statistical Association* 111(513), 253–265.
- Cai, T. T., C.-H. Zhang, and H. H. Zhou (2010). Optimal rates of convergence for covariance matrix estimation. *The Annals of Statistics* 38(4), 2118–2144.
- Cai, T. T. and H. H. Zhou (2012a). Minimax estimation of large covariance matrices under 1-norm. *Statistica Sinica* 22(4), 1319–1349.
- Cai, T. T. and H. H. Zhou (2012b). Optimal rates of convergence for sparse covariance matrix estimation. *The Annals of Statistics* 40(5), 2389–2420.
- Cao, X., K. Khare, and M. Ghosh (2016). Posterior graph selection and estimation consistency for high-dimensional bayesian dag models. *arXiv:1611.01205*.
- Fan, J., Y. Fan, and J. Lv (2008). High dimensional covariance matrix estimation using a factor model. *Journal of Econometrics* 147(1), 186–197.
- Fan, J., P. Rigollet, and W. Wang (2015). Estimation of functionals of sparse covariance matrices. *Annals of statistics* 43(6), 2706.
- Gao, C. and H. H. Zhou (2015). Rate-optimal posterior contraction for sparse pca. *The Annals of Statistics* 43(2), 785–818.
- Gao, C. and H. H. Zhou (2016). Bernstein-von mises theorems for functionals of the covariance

REFERENCES38

- matrix. *Electronic Journal of Statistics* 10(2), 1751–1806.
- Ghosal, S., J. K. Ghosh, and A. W. van der Vaart (2000). Convergence rates of posterior distributions. *Annals of Statistics* 28(2), 500–531.
- Ghosal, S. and A. van der Vaart (2007). Posterior convergence rates of dirichlet mixtures at smooth densities. *The Annals of Statistics* 35(2), 697–723.
- Hu, A. and S. Negahban (2017). Minimax estimation of bandable precision matrices. In *Advances in Neural Information Processing Systems*, pp. 4895–4903.
- Johnstone, I. M. and A. Y. Lu (2009). On consistency and sparsity for principal components analysis in high dimensions. *Journal of the American Statistical Association* 104(486), 682–693.
- Khare, K., S. Oh, S. Rahman, and B. Rajaratnam (2016). A convex framework for high-dimensional sparse cholesky based covariance estimation. *arXiv preprint arXiv:1610.02436*.
- Koller, D. and N. Friedman (2009). *Probabilistic graphical models: principles and techniques*. MIT press.
- Lauritzen, S. L. (1996). *Graphical models*, Volume 17. Clarendon Press.
- Lee, K. and J. Lee (2018). Optimal Bayesian Minimax Rates for Unconstrained Large Covariance Matrices. *Bayesian Analysis* 13(4), 1211–1229.
- Liu, Y. and Z. Ren (2017, December). Minimax Estimation of Large Precision Matrices with Bandable Cholesky Factor. *ArXiv e-prints*.

REFERENCES39

- Pati, D., A. Bhattacharya, N. S. Pillai, and D. Dunson (2014). Posterior contraction in sparse bayesian factor models for massive covariance matrices. *The Annals of Statistics* 42(3), 1102–1130.
- Rütimann, P. and P. Bühlmann (2009). High dimensional sparse covariance estimation via directed acyclic graphs. *Electronic Journal of Statistics* 3, 1133–1160.
- Scott, S. L., A. W. Blocker, F. V. Bonassi, H. A. Chipman, E. I. George, and R. E. McCulloch (2016). Bayes and big data: The consensus monte carlo algorithm. *International Journal of Management Science and Engineering Management* 11(2), 78–88.
- Shojaie, A. and G. Michailidis (2010). Penalized likelihood methods for estimation of sparse high-dimensional directed acyclic graphs. *Biometrika* 97(3), 519–538.
- Verzelen, N. (2010). Adaptive estimation of covariance matrices via cholesky decomposition. *Electronic Journal of Statistics* 4, 1113–1150.
- Xiang, R., K. Khare, and M. Ghosh (2015). High dimensional posterior convergence rates for decomposable graphical models. *Electronic Journal of Statistics* 9(2), 2828–2854.
- Xue, L. and H. Zou (2013). Minimax optimal estimation of general bandable covariance matrices. *Journal of Multivariate Analysis* 116, 45–51.

The University of Notre Dame

E-mail: (leekjstat@gmail.com)

Seoul National University

REFERENCES⁴⁰

E-mail: (leejyc@gmail.com)

Statistica Sinica